

## Design of a visible light communication system using universal software radio peripheral

Rodrigo F. Miranda\* Carlos H. Barriquello\*\* Vitalio A. Reguera\*\*\*  
Lucas Teixeira\*\*\*\* Marco A. D. Costa† Djeisson H. Thomas‡

\* Universidade Federal de Santa Maria (e-mail: rodrigo.fmir@gmail.com).  
\*\* Universidade Federal de Santa Maria (e-mail: barriquello@gmail.com).  
\*\*\* Universidade Federal de Santa Maria (e-mail: vitalio.reguera@ufsm.br).  
\*\*\*\* Universidade Federal de Santa Maria (e-mail: lucas.teixeira@ufsm.br).  
† Universidade Federal de Santa Maria (e-mail: marcodc@gedre.ufsm.br).  
‡ Universidade Federal de Santa Maria (e-mail: djeisson.thomas@ufsm.br).

**Abstract:** The main target of this paper is to present the development steps of a Visible Light Communication (VLC) system applied to Solid-State Lighting (SSL) with frequency suitable to an Universal Software Radio Peripheral (USRP). The goal here is to establish a testbed prototype according to the frequency response limits of the hardware used, to make possible studies of VLC applications with real-time evaluation of the performance metrics.

**Keywords:** GNU Radio, SSL, USRP, VLC.

### 1. INTRODUCTION

Visible Light Communication (VLC) technology based on Solid-State Lighting (SSL) allows new solutions for problems usually found in traditional Radio Frequency (RF) communications, more specifically to the crowded RF spectrum. Some important advantages are related to high data rate transmission and broadband solutions, as well as, security aspects, unlicensed channels, suitable for integration with 5G. Moreover, VLC is electromagnetically immune to interference generated by RF devices, which together with other technical characteristics like the wide bandwidth available, makes VLC a promising technology for critical communication environments (Karunatilaka et al., 2015; Oyewobi et al., 2022).

The digital information is carried by the light without impairing the lighting function and under a high data rate fast enough to be imperceptible to human eyes, avoiding flicker effects (Teixeira et al., 2021). The capability and flexibility of a Universal Software Radio Peripheral (USRP) hardware allows users to deploy a typical VLC communication system with the GNU Radio (GR) framework in a convenience computer or an embedded system (Van et al., 2014).

There are two important standards being development to support VLC: IEEE 802.11.bb and International Telecommunication Union - Telecommunication Standardization Sector (ITU-T G.9991), where the former focuses the commercial applications and the later focus the industry field, being both of them in constant evolution with recommendations directives in Physical Layer (PHY) and Medium Access Control (MAC) protocols (Purwita and Haas, 2020).

\* This study was financed in part by the Coordenação de Aperfeiçoamento de Pessoal de Nível Superior – Brasil (CAPES/PROEX) – Finance code 001. Special thanks to the Group of Intelligence in Lighting (GEDRE) where this work was developed.

Therefore, and considering its technical characteristics previously exposed, a testbed prototype of VLC based on the GR framework is proposed, to enable the evaluation of applications under real-time performance metrics.

### 2. VLC SYSTEM BACKGROUND

A VLC system model is depicted in Fig. 1.

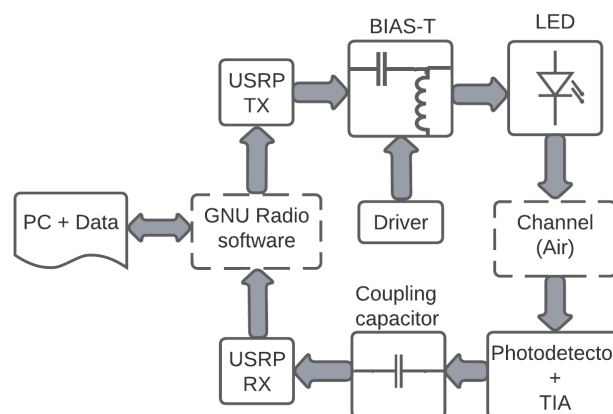


Fig. 1. VLC system of this paper.

At the beginning of the communication system, a data stream generated by a Personal Computer (PC) is coupled to the GR by its software framework. This data is used to modulate a high frequency microwave carrier and it is sent by Universal Software Radio Peripheral Transmitter (USRP-TX) to be added to a DC biased through a bias-T circuit to the SSL device. The optical carrier propagates in the free space before to reach the photodiode (PD), which output photocurrent is coupled

to a Trans-Impedance Amplifier (TIA), enabling the higher-level voltage signal to be filtered by the coupling capacitor to reduce the DC level. Therefore, the filtered signal is received by the USRP-RX and the transmitted data can be recovered by PC, under GR software supervision and decoding. All diagram blocks are bandwidth compatible. One of the considerations to design a VLC system is the propagation link displayed in Fig. 2, that may be classified into two categories: Line-Of-Sight (LOS) link and Non-Line-Of-Sight (NLOS) link. Since the power of the LOS path dominates and the power of the reflected paths is much lower, a LOS wireless system usually has a higher power efficiency. We will consider only LOS link as it is a common text scenario for experimental VLC links. So, considering the link with an angle  $\varphi$  regarding a normal line to the center of the light source, and the frequency response relatively flat near to DC we can express the DC channel gain as (1).

$$H_{LOS} = \frac{(m+1) \cdot A}{2\pi \cdot d^2} \cdot \cos^m(\phi) \cdot \cos(\varphi) \quad (1)$$

The coefficient  $(m+1)A/2\pi d^2$  ensures that the radiant intensity integration over the surface of a hemisphere equals the total optical power. Furthermore,  $m$  is the order of Lambertian emission given by (2), that depends on light source half-angle  $\varphi_{1/2}$  (Fahamuel et al., 2013; Chaurasia et al., 2020). So, the DC gain depends on the distance  $d$  between the transmitter and the receiver, the irradiation angle  $\varphi$  and the incident irradiation angle  $\phi$ .

$$m = \frac{-\ln(2)}{\ln(\cos(\varphi_{1/2}))} \quad (2)$$

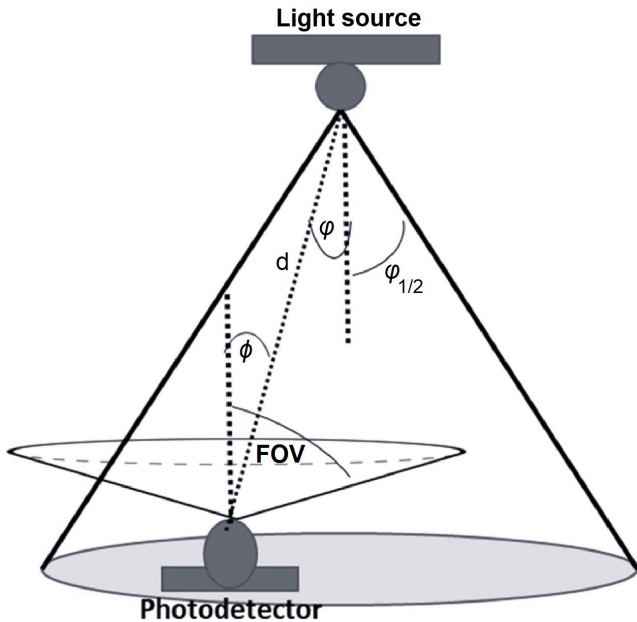


Fig. 2. Ray diagram, edited from: Khalifeh et al. (2018).

Even though these aspects depend on the distance and angles between the optical emitter and receiver, they are not critical factors to the current prototype design. Therefore, only dynamics limitations to VLC system will be considered, especially those related to LED and PD, which are detailed in Brum et al. (2018).

### 3. DESIGN OF THE VLC SYSTEM

The most important choice to start a VLC design may be the definition of the application. The optimal components of an application that requires mobility and energy saving like an outdoor use are very different from applications that use only indoor or long-distance transmission. Even though the application being indoor or outdoor, the proposed prototype is intended to support deeper research regarding the VLC system performance, including, but not limited to, the following topics: signal processing algorithms, codifications, drivers, filters, modulation formats, security issues, synchronism and nonlinear distortion. According to the prototype topology proposed, the evaluation of these aspects is limited to a Single-Input and Single-Output (SISO) VLC scheme. The capacity given by the USRP, considered the BW bottleneck, will define the theoretical channel capacity of this work, which is ruled by Shannon's noisy-channel theorem (Shannon, 1949) in equation (3).

$$C = BW \cdot \log_2(1 + SNR) \quad (3)$$

Where  $C$  is the channel capacity in *bits/sec*.

#### 3.1 The choice of PD

The commercial PD have many trade-offs among its parameters that affect the target behavior, and we need to select some of these parameters according to requirements established during the design process (Fuada et al., 2017). In this section are listed the most important aspects to choose an off-the-shelf component.

**Response time.** Usually in PIN PD we can use the pulse response time  $\tau$  or the cutoff frequency  $f_c$  to characterize the dynamic response of the PD to the high-speed modulated optical signal. If we consider that the PD has the same pulse leading and lagging edge, close to functions  $[1 - \exp(-t/\tau_0)]$  and  $[\exp(-t/\tau_0)]$  and time constant  $\tau_0$  (which represent the RC constant of photodetector), the resulting impulse response time is:

$$t = t_r = t_f = 2.2 \cdot \tau_0 \quad (4)$$

For a sinusoidal modulation signal with a constant amplitude and frequency  $\omega = 2\pi f$ , being the cutoff frequency  $f_c$  defined when the light-generated current  $I(\omega)$  decreases 3 dB. So, the cutoff frequency is limited by the RC time constant of the circuit:

$$f_c = \frac{1}{2\pi \cdot R_t \cdot C_d} \quad (5)$$

Where  $R_t$  is the sum of all the series resistance and the load resistance of the PD, while  $C_d$  is the sum of the junction capacitance  $C_j$  and the distributed capacitance. These intrinsic parameters have a behavior like a low-pass filter (Hoeher, 2019).

**Bandwidth.** The choice of the PD also requires a maximum active area  $A_f$  (photosensitive part of PD) to enable it to detect the maximum incident optical power ( $P_{in}$ ) and to increase the distance between the emitter and receiver. Using (6) it is possible to choose a PD with maximum  $A_f$  since the requirements of  $f_c$  can be reached through the RC time constant.

$$BW = \frac{1}{2\pi \cdot (\tau_r + \tau_{RC})} \quad (6)$$

Where  $\tau_r$  and  $\tau_{RC}$  represent the transmission time and discharge time, respectively. However, a PD with a large  $A_f$  will be more susceptible to interference from other light sources, degrading the Signal-to-Noise Ratio (SNR) and also the Bit Error Rate (BER). In such cases, the VLC system performance can be

improved using alternative processing methods, such as signal equalization or error detection and correction codes methods (Saha et al., 2012; Gour and Kumar, 2016; Ghassemlooy et al., 2013).

**Noise Equivalent Power (NEP).** The NEP is the input signal power that results in a SNR of one with 1Hz of BW, which is equivalent to an integration time of 0.5s (Hoeher, 2019). The NEP should also be as small as possible as it is a metric for the sensitivity of a PD:

$$NEP = \frac{IncidentEnergy \cdot A_f}{SNR \cdot \sqrt{\Delta f}} \quad (7)$$

In (7) the NEP increases as much as the  $A_f$  grows, but decreases with the SNR. We can express the SNR as in (8), if we assume a optical channel with Additive White Gaussian Noise (AWGN) model:

$$SNR = \frac{(R_\lambda \cdot P_r)^2}{\sigma_{shot}^2 + \sigma_{thermal}^2} \quad (8)$$

Where  $R_\lambda$  is the PD responsivity,  $P_r$  is the average received optical power,  $\sigma_{shot}^2$  and  $\sigma_{thermal}^2$  are respectively shot and thermal noise of the PD. Taking into account these parameters, a good choice is the device PDA10A2 from ThorLabs, whose specifications are displayed in Table 1. Is important to emphasize that this device is not a photodiode, but it is a photoreceptor, since it accomplishes all the reception functions, including amplification.

Table 1. PD specifications.

Parameter	Value
Responsivity at 730 nm	0.44A/W
Area ( $A_f$ )	0.8mm <sup>2</sup>
Small Signal Bandwidth	150MHz
Transimpedance Gain	1 · 10 <sup>4</sup> V/A (to Hi-Z) 5 · 10 <sup>3</sup> V/A (to 50Ω)
NEP at 730nm	2.92 · 10 <sup>-11</sup> W/√Hz

### 3.2 The choice of the light source

Considering the frequency response requirement, the proposed VLC prototype is limited to use only three types of SSLs: Laser Diodes (LD),  $\mu$ -LED, and non-phosphor coated LED, whose BW are respectively: Up to tens of GHz, about 300MHz and up to tens of MHz (Mapunda et al., 2020; Hranilovic, 2005). The phosphor-coated white LED was disregarded because it has a BW limited to 5MHz (Li et al., 2014). In the LED-based transmitter, the maximum modulation frequency is limited by the LED's BW, which depends on device construction (material and geometry) (Perera, 2020). Furthermore, another operation condition related to the maximum modulation frequency is the modulation depth:

$$m_d = \frac{\Delta I}{I_0} \quad (9)$$

Where  $I_0$  is the bias current and  $\Delta I$  is the current variation related to the modulating signal. The larger the modulation depth is, it is easier for the receiver to effectively detect the signal, at the expense of a narrow BW. Therefore, the modulation BW is part of the definition of the transmission rate and consequently the VLC channel capacity in the system (Wu et al., 2018). However, this aspect does not affect the choice of our LED, since the modulation depth is changeable. There are more influencing factors that affect the frequency response of the

LED, current density, LED chip size and package type (Luan and Qian, 2017). Thus, a good choice is a LED with size and package as small as possible, as well, with high current density. However, considering the availability of components and the BW requirement, the choice was the RGB LEDs. Specifically, the choice was a red LED from Cree® model XLamp® XR-C.

### 3.3 The choose of bias-T

The bias-T circuit consists of a passive device with a RF input signal and another input for biasing, while the output delivers the combined RF and bias signals, as depicted in Fig. 3. At the RF input the bias-T should provide broadband frequency coverage and high impedance at low frequencies. On the other hand, at the bias input, it must provide strong attenuation for high frequency signals with no distortion of low frequencies. This requires that the load impedance must be matched to the bias-T output impedance, otherwise frequency selectivity becomes load dependent (Ghassemlooy et al., 2017).

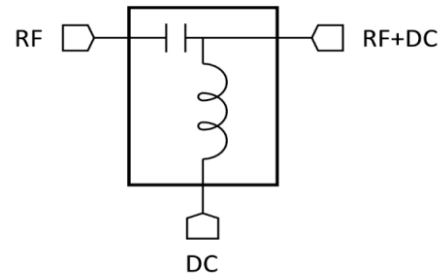


Fig. 3. Bias-T circuit.

Therefore, to calculate the bias-T components the lower frequency limit was limited by the USRP operational range, 10MHz. To define the capacitor value, the equation of the capacitive reactance was employed (10):

$$C = \frac{1}{2\pi \cdot f \cdot X_C} \quad (10)$$

Where  $f$  represents the lower frequency limit and  $X_C$  is the capacitive reactance. The value of  $X_C$  follows the ratio 1 : 100 regarding the load resistance, as can be seen in (11), which specifies the low RF impedance limit:

$$X_C = \frac{R_{eq}}{100} \quad (11)$$

The  $R_{eq}$  represents the equivalent resistance of the load.

Similarly, the inductor value was defined using the equation of the inductive reactance (12).

$$L = \frac{X_L}{2\pi \cdot f} \quad (12)$$

In this case, the value of  $X_L$  follows the ratio 100 : 1 regarding  $R_{eq}$ , as can be seen in (13), which specifies the lower impedance limit.

$$X_L = R_{eq} \cdot 100 \quad (13)$$

In case it is necessary to increase the impedance of the inductor path without changing its value, it is possible to add a ferrite bead in series, since this component has a small DC resistance but a high impedance for RF frequencies Hicks and Erickson (2008).

There other practical details that will affect the bias-T project is the inductor saturation current and the self-resonant frequency of the inductor and capacitor, which can result in an unexpected behavior of this circuit. In this paper we choose to avoid the resonant frequency according to the datasheet of the components used.

Therefore, two bias-T circuit boards were mounted, the first to be applied to only one red LED while the second one can be potentially applied to 48 red LEDs associated in series. The parameters of the two bias-T are displayed at Table 2.

Table 2. Bias-T parameters.

Bias-T	1	2
Capacitor	2.2 $\mu F$	47 $\mu F$
Inductor	1 $\mu H$	66 $\mu H$
R bead	600 $\Omega$	600 $\Omega$
SRF (L)	90MHz	8MHz
I (sat.)	8A	4.2A

### 3.4 USRP

The USRP TX and RX specifications are shown in Tables 3 and 4. The concern about the USRP is basically to fit the input

Table 3. USRP transmitter specifications.

Parameter	Value
Frequency range	10MHz to 6GHz
Maximum output power in watts	50mW to 100mW
Maximum output power in dBm	17dBm to 20dBm
Maximum instantaneous real-time BW	160MHz
Maximum I/Q sample rate	200MS/s
Digital-to-analog converter resolution	16bit

Table 4. USRP receiver specifications.

Parameter	Value
Frequency range	10MHz to 6GHz
Maximum input power in dBm	-15dBm
Maximum instantaneous real-time BW	160MHz
Maximum I/Q sample rate	200MS/s
Noise figure	5dB to 7dB
Digital-to-analog converter resolution	14bit

and output power requirements, since this device is the BW bottleneck of the system. In Molla et al. (2022) the authors compare many USRP devices with wireless technologies. Considering those results, the platform employed to build the proposed prototype (USRP X310-based) reached one between the highest bit rates, i.e., 1906, 1Mbit/s, under the IEEE 802.11ac standard. The hardware and software components of the system proposed are described in Table 5.

Table 5. Hardware and Software Components.

Hardware/Software	Name/Version
OS	UBUNTU 20.04
GNURADIO	3.9.5.0 (Python 3.8.10)
UHD	3.15.0.0-2build5
USRP Transmitter	USRP2499R
USRP Receiver	USRP2499R

### 3.5 GNU Radio and communication standards

The choice of GNU Radio is due to the fact that it is an open-source signal processing framework that supports the hardware connectivity in the USRP platform. Additionally, the GNU Radio represents a versatile solution because of its generous library, being adaptable according to each project of software radio system.

The communication standard of physical and MAC layers of VLC is being developed by the IEEE 802.11bb task group on light communications, which are submitting changes based on IEEE 802.11a. This standard was first adopted in 1999, and it defines requirements for an Orthogonal Frequency-Division Multiplexing (OFDM)-based communication system. The main difference of IEEE 802.11bb and others standards is related to the focus on delivering a mobile and networked solution of light-based communication systems, which use off-the-shelf Wi-Fi chipsets (Purwita and Haas, 2020). Moreover, this standard allows us to set a 160MHz BW channel, which is very convenient to our system. Figs. 4 and 5 presents, respectively, the transmission and reception block of GR which employs an OFDM modulation technique according to the IEEE 802.11a parameters (see Table 6). The block diagrams implemented are adapted from GitHub (2022) and its flow-graph are detailed by Sowjanya and Satyanarayana (2019), and used to validate the proposed VLC system. The OFDM technique uses BPSK and QPSK modulation for cyclic prefix and payload parts of a symbol respectively.

Table 6. OFDM PHY Parameters (IEEE 802.11a).

Parameter	Value
BW	20MHz
OFDM subcarrier	64
Subcarrier spacing	312KHz
OFDM symbol time	4 $\mu s$
Guard time	1.6 $\mu s$
Comb-pilot spacing	4.4MHz
Center frequency	2.2Ghz

## 4. OTHERS PERFORMANCES CONSIDERATIONS

Most of the papers used in this study use OFDM with light Intensity Modulation (IM) on LEDs. Because of the natural behavior of the light, it is not possible to obtain negative numbers by IM application. So, it is necessary to add a DC signal on the OFDM or use asymmetric clipping to fix that, a technique called Asymmetrically Clipped Optical OFDM (ACO-OFDM). However, the required amplitude of DC bias results in a high Peak-to-Average Power Ratio (PAPR) in the OFDM symbols, which can turn the system power inefficient (Armstrong and Schmidt, 2008).

One partial solution for the problem above is described in Fernando et al. (2011), which compares a modified Flip-OFDM (unipolar OFDM) to ACO-OFDM. They conclude that both have similar SNR values, but with Flip-OFDM use it, possible to save hardware computation efforts, and consequently, to save energy. Energy saving is an important issue in optical OFDM based systems, but also the nonlinearity of the LEDs is specially affected in high PAPR transmission path, because the amplitude distortion during high power and lower peak clipping lead to significant signal degradation (Chi, 2018).

Another feature of OFDM that can be optimized is related to the modulation order, that can be adaptively selected at each

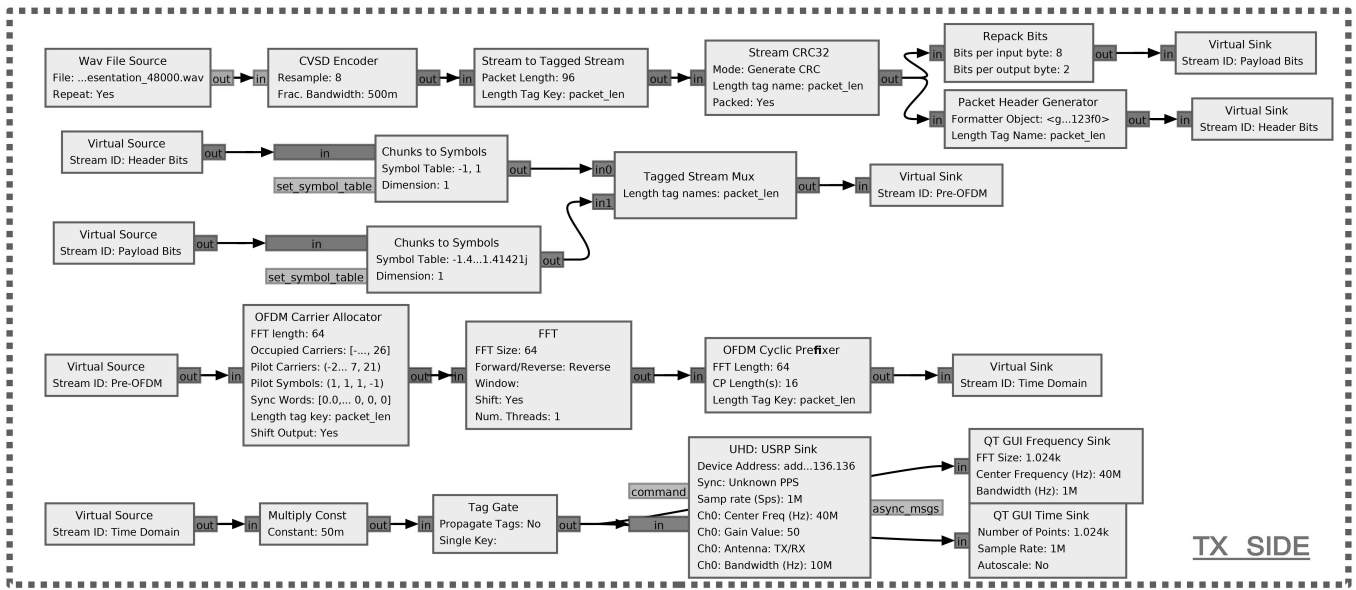


Fig. 4. Transmission diagram in GNU Radio.

subcarrier to maximize the data rate at a target BER (Bian et al., 2019). The SNR estimation is required at each subcarrier to improve the data transmission quality. The channel response and available SNR at each subcarrier were calculated using pilots by several OFDM blocks.

In Chen et al. (2019) the authors use the photo-electro-thermal (PET) theory to evaluate the performance of a VLC system. They conclude that the SNR variation about electro-thermal effects dependence of LED and LD are "substantial" in specific scenarios and that it is an important consideration to achieve

desirable performances. Therefore, this is a future consideration to our design.

## 5. EXPERIMENTAL SETUP AND RESULTS

To validate the proposed system, a prototype was implemented as depicted in Fig. 6. The equipment used in this setup is shown in Table 7. A router is used to connect the data from the PC to USRPs. Three coaxial cables are used to connect the USRP to the bias-T circuit and the coupling capacitor. The channel is the free space between red LED and PD plus TIA.

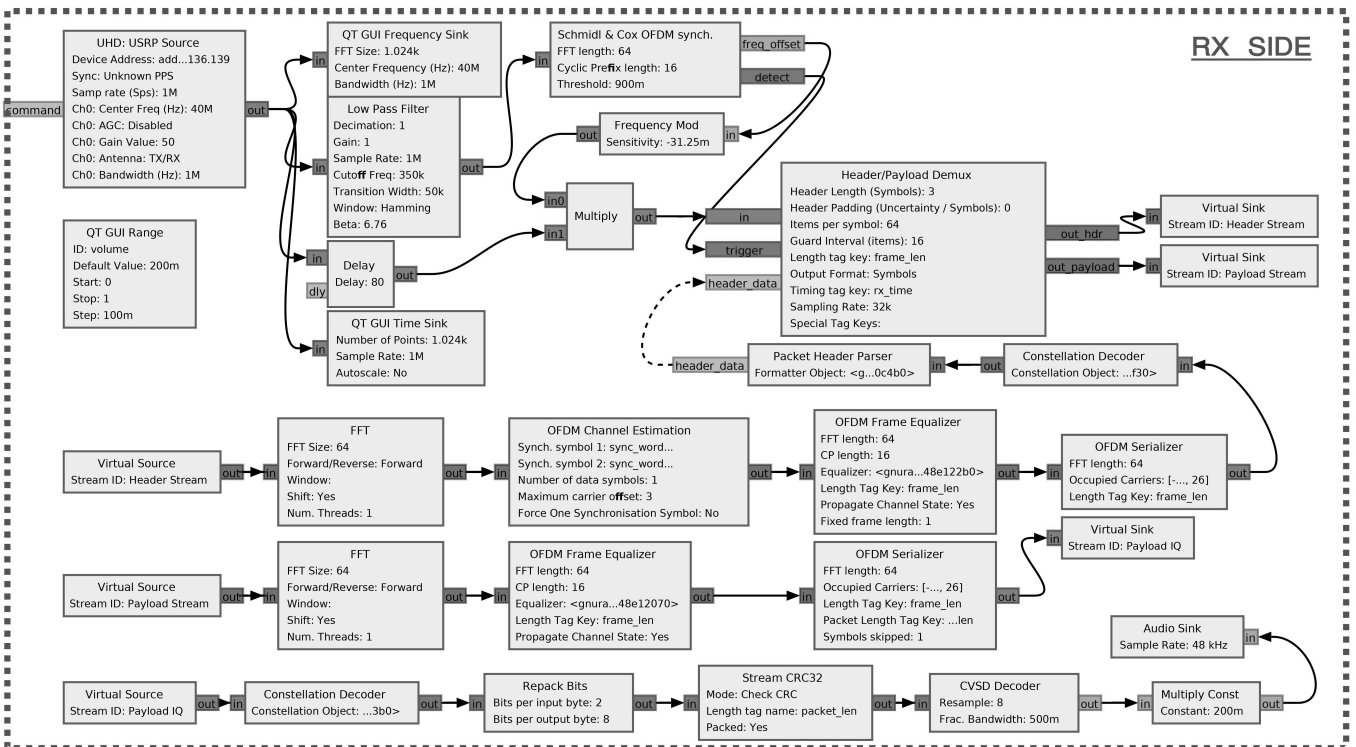


Fig. 5. Receiver diagram in GNU Radio.

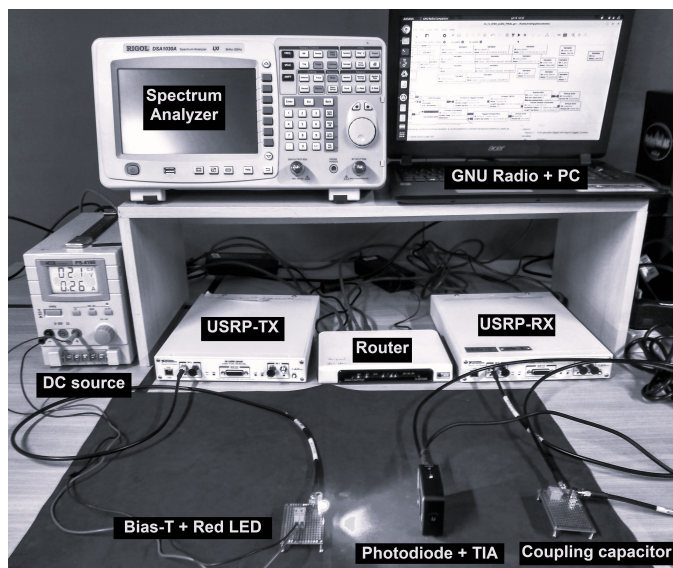


Fig. 6. Testbed implemented.

Table 7. List of equipment.

Equipment	Model
Spectrum analyzer	Rigol DSA1030A
USRP	National Instruments 2944
PD	ThorLabs PDA10A2
Router	TP-LINK WR1043ND
PC	Acer Aspire ES1-572-37PZ
DC source	ICEL PS-4100
Red LED	Cree XLamp XR-C
Coaxial cable SMA-SMA	NI 156923A-01

The proposed methodology was intended to realize a real-time evaluation of the performance metrics. However, during the tests, the host machine (PC) could not keep up with the requested sample rates and with the evaluations tools of GNU Radio (Ettus Research, 2022).

Nevertheless, with the spectrum analyzer it was possible to measure the SNR value of the PD output signal. An audio file (\*.wav) with 3min of duration was sent by USRP-T in real-time with 20MHz BW. The distance between emitter and receiver was 10cm. The output signal, after the coupling capacitor is depicted in Fig. 7.

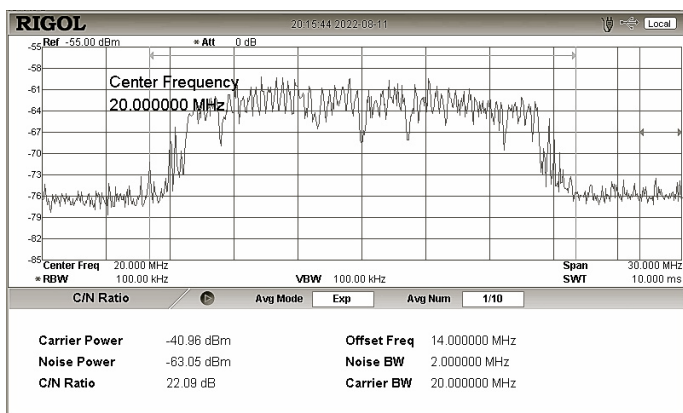


Fig. 7. Signal power spectrum.

The vertical axis shows the dBm value in 3dBm/div. while the horizontal axis shows the frequency with 3MHz/div. The

first horizontal arrow is the carrier BW, and the second is the noise BW. The carrier frequency (Center Frequency) is 20MHz, in a span of 10MHz to 30MHz, which is the lower limit of the USRPs. The SNR measured was 22dB, a value considered enough for data networks, when compared to the performance of the traditional wireless networks (Cisco Meraki, 2020).

## 6. CONCLUSION

We know that different environments can affect the overall frequency response of the communication system and make it frequency dependent, for example, ambient light sources, unforeseen frequency response of devices and the optical channel itself may affect the dynamic behavior of the system.

An audio file was successfully transferred in real-time through a light channel and measured the SNR value, which is a critical parameter of a VLC system. Nonetheless, only the bias-T for one LED was employed and cannot evaluate the SNR in the upper limits. The processing limitation of the PC gave us a sampling frequency of 20MS/s in accordance with the BW of RGB LED, which without additional circuits could not exceed tens of MHz.

However, this work gives a wide view of the design steps rules of each block of the VLC system, which can provide a large bandwidth to evaluate the overall performance of the communication. With the exception of the LED, the BW limit of the system is equivalent to all devices explored and with latest VLC standards, which makes it very convenient to develop applications based on these standards, allowing us to achieve several Gbits of data rate. Moreover, the choice of the USRP and its configuration via GNU Radio allows changing the communication parameters easily, enabling to explore experimentally the VLC potential over a variety of application scenarios.

## REFERENCES

- Armstrong, J. and Schmidt, B.J. (2008). Comparison of asymmetrically clipped optical OFDM and DC-biased optical OFDM in AWGN. *IEEE Commun. Lett.*, 12(5), 343–345.
- Bian, R., Tavakkolnia, I., and Haas, H. (2019). 15.73 Gb/s Visible Light Communication with Off-the-Shelf LEDs. *J. Light. Technol.*, 37(10), 2418–2424.
- Brum, J.P.S., Loose, F., Teixeira, L., Costa, M.A.D., and Reguera, V.A. (2018). Modelagem da Resposta em Frequência de um Sistema de Comunicação por Luz Visível. In *11<sup>o</sup> Semin. Power Electron. Control*, 10.
- Chaurasia, A., Sharma, M., Akansha, Garg, A., and Rani, R. (2020). Statistical analysis of SNR and optical power distribution in an indoor VLC System. *J. Phys. Conf. Ser.*, 1706(1).
- Chen, H., Lee, A.T., Tan, S.C., and Hui, S.Y. (2019). Electrical and Thermal Effects of Light-Emitting Diodes on Signal-to-Noise Ratio in Visible Light Communication. *IEEE Trans. Ind. Electron.*, 66(4), 2785–2794.
- Chi, N. (2018). *LED-Based Visible Light Communications*. Springer.
- Cisco Meraki (2020). *Signal-to-Noise Ratio (SNR) and Wireless Signal Strength*. URL [https://documentation.meraki.com/@api/deki/pages/1322/pdf/Signal-to-Noise2bRatio\(SNR\)bandWirelessSignaStrength.pdf](https://documentation.meraki.com/@api/deki/pages/1322/pdf/Signal-to-Noise2bRatio(SNR)bandWirelessSignaStrength.pdf).

- Ettus Research (2022). *USRP Hardware Driver and USRP Manual Version: 4.2.0.0-143-g2ad30980f*. URL [https://files.ettus.com/manual/page\\_general.html](https://files.ettus.com/manual/page_general.html).
- Fahamuel, P., Thompson, J., and Haas, H. (2013). Study, analysis and application of optical OFDM, single carrier (SC) and MIMO in intensity modulation direct detection (IM/DD). *IET Conf. Publ.*, 2013. doi:10.1049/cp.2013.2050.
- Fernando, N., Hong, Y., and Viterbo, E. (2011). Flip-OFDM for optical wireless communications. *2011 IEEE Inf. Theory Work. ITW 2011*, 5–9.
- Fuada, S., Pratama, A., and Adiono, T. (2017). Analysis of Received Power Characteristics of Commercial Photodiodes in Indoor Los Channel Visible Light Communication. *Int. J. Adv. Comput. Sci. Appl.*, 8(7), 164–172.
- Ghassemlooy, Z., Popoola, W., and Rajbhandari, S. (2013). *Optical wireless communications: System and channel modelling with MATLAB®*. CRC Press.
- Ghassemlooy, Z., Alves, L.N., Zvánovec, S., and Khalighi, M.A. (2017). *Visible Light Communications Theory and Applications*. CRC Press.
- GitHub (2022). Gnu radio public repository. <https://github.com/gnuradio/gnuradio/tree/main/gr-digital/examples/ofdm>.
- Gour, S. and Kumar, S. (2016). Reduction of optical background noise impact in light-emitting diode (LED)-based optical wireless communication systems by Hadamard Codes. *Adv. Intell. Syst. Comput.*, 397, 919–927.
- Hicks, B. and Erickson, B. (2008). Bias-T Design Considerations for the LWA. Technical report.
- Hoeher, P.A. (2019). *Visible Light Communications Theoretical and Practical Foundations*. Hanser Publications.
- Hranilovic, S. (2005). *Wireless optical communication systems*. Springer.
- Karunatilaka, D., Zafar, F., Kalavally, V., and Parthiban, R. (2015). LED based indoor visible light communications: State of the art. *IEEE Commun. Surv. Tutorials*, 17(3), 1649–1678.
- Khalifeh, A.F., AlFasfous, N., Theodory, R., Giha, S., and Darabkh, K.A. (2018). An experimental evaluation and prototyping for visible light communication. *Comput. Electr. Eng.*, 72, 248–265.
- Li, H., Chen, X., Huang, B., Tang, D., and Chen, H. (2014). High bandwidth visible light communications based on a post-equalization circuit. *IEEE Photonics Technol. Lett.*, 26(2), 119–122.
- Luan, T. and Qian, K. (2017). Research on influencing factors of LED frequency response. *AIP Conf. Proc.*, 1864(August 2017).
- Mapunda, G.A., Ramogomana, R., Marata, L., Basutli, B., Khan, A.S., and Chuma, J.M. (2020). Indoor Visible Light Communication: A Tutorial and Survey. *Wirel. Commun. Mob. Comput.*, 2020.
- Molla, D.M., Badis, H., George, L., and Berbineau, M. (2022). Software Defined Radio Platforms for Wireless Technologies. *IEEE Access*, 10, 26203–26229.
- Oyewobi, S.S., Djouani, K., and Kurien, A.M. (2022). Visible Light Communications for Internet of Things: Prospects and Approaches, Challenges, Solutions and Future Directions. *Technologies*, 10(1), 28.
- Perera, M.A.N. (2020). *Design and implementation of a light-based IoT (LIoT) node using printed electronics*. Ph.D. thesis, University of Oulu.
- Purwita, A.A. and Haas, H. (2020). IQ-WDM for IEEE 802.11bb-based LiFi. In *IEEE Wirel. Commun. Netw. Conf.* Seoul, Korea (South).
- Saha, N., Mondal, R.K., Le, N.T., and Jang, Y.M. (2012). Mitigation of interference using OFDM in visible light communication. *Int. Conf. ICT Converg.*, 159–162.
- Shannon, C.E. (1949). Communication in the Presence of Noise. *Proc. IRE*, 37(1), 10–21.
- Sowjanya, P. and Satyanarayana, P. (2019). Real-time data transfer based on software defined radio technique using gnu radio/usrp. *Int. J. Eng. Adv. Technol.*, 9(1), 279–288.
- Teixeira, L., Loose, F., Barriquello, C.H., Reguera, V.A., Costa, M.A.D., and Alonso, J.M. (2021). On energy efficiency of visible light communication systems. *IEEE J. Emerg. Sel. Top. Power Electron.*, 9(5), 6396–6407.
- Van, D.N., Anh, T.N., Ngoc, T.T., Nguyen, V.D., Jeon, B., and Nguyen, T.H. (2014). A real-time COFDM transmission system based on the GNU Radio - USRP N210 platform. *Proc. 8th Int. Conf. Ubiquitous Inf. Manag. Commun. ICUIMC 2014*, 1–5.
- Wu, Z.Y., Liu, X.Y., Wang, J.S., and Wang, J. (2018). Modulation index dependence of intensity modulation bandwidth in visible light communications. *Opt. Lett.*, 43(19), 4570–4573.